AMERICAN SOCIETY FOR MICROBIOLOGY | mBio®

Check for updates

Bacillus anthracis Responds to Targocil-Induced Envelope Damage through EdsRS Activation of Cardiolipin Synthesis

Clare L. Laut,[a,b] William J. Perry,[c,d] Alexander L. Metzger,[e] Andy Weiss,[a,b] Devin L. Stauff,[e] Suzanne Walker,[f] Richard M. Caprioli,[c,d,g,h,i] Eric P. Skaar[a,b]

[a]Department of Pathology, Microbiology, and Immunology, Vanderbilt University Medical Center, Nashville, Tennessee, USA

[b]Vanderbilt Institute for Infection, Immunology, and Inflammation, Vanderbilt University Medical Center, Nashville, Tennessee, USA

[c]Mass Spectrometry Research Center, Vanderbilt University, Nashville, Tennessee, USA

[d]Department of Chemistry, Vanderbilt University, Nashville, Tennessee, USA

[e]Department of Biology, Grove City College, Grove City, Pennsylvania, USA

[f]Department of Microbiology and Molecular Genetics, Harvard Medical School, Boston, Massachusetts, USA

[g]Department of Biochemistry, Vanderbilt University, Nashville, Tennessee, USA

[h]Department of Pharmacology, Vanderbilt University, Nashville, Tennessee, USA

[i]Department of Medicine, Vanderbilt University Medical Center, Nashville, Tennessee, USA

ABSTRACT *Bacillus anthracis* is a spore-forming bacterium that causes devastating infections and has been used as a bioterror agent. This pathogen can survive hostile environments through the signaling activity of two-component systems, which couple environmental sensing with transcriptional activation to initiate a coordinated response to stress. In this work, we describe the identification of a two-component system, EdsRS, which mediates the *B. anthracis* response to the antimicrobial compound targocil. Targocil is a cell envelope-targeting compound that is toxic to *B. anthracis* at high concentrations. Exposure to targocil causes damage to the cellular barrier and activates EdsRS to induce expression of a previously uncharacterized cardiolipin synthase, which we have named ClsT. Both EdsRS and ClsT are required for protection against targocil-dependent damage. Induction of *clsT* by EdsRS during targocil treatment results in an increase in cardiolipin levels, which protects *B. anthracis* from envelope damage. Together, these results reveal that a two-component system signaling response to an envelope-targeting antimicrobial induces production of a phospholipid associated with stabilization of the membrane. Cardiolipin is then used to repair envelope damage and promote *B. anthracis* viability.

IMPORTANCE Compromising the integrity of the bacterial cell barrier is a common action of antimicrobials. Targocil is an antimicrobial that is active against the bacterial envelope. We hypothesized that *Bacillus anthracis*, a potential weapon of bioterror, senses and responds to targocil to alleviate targocil-dependent cell damage. Here, we show that targocil treatment increases the permeability of the cellular envelope and is particularly toxic to *B. anthracis* spores during outgrowth. In vegetative cells, two-component system signaling through EdsRS is activated by targocil. This results in an increase in the production of cardiolipin via a cardiolipin synthase, ClsT, which restores the loss of barrier function, thereby reducing the effectiveness of targocil. By elucidating the *B. anthracis* response to targocil, we have uncovered an intrinsic mechanism that this pathogen employs to resist toxicity and have revealed therapeutic targets that are important for bacterial defense against structural damage.

KEYWORDS *Bacillus anthracis*, antimicrobial agents, cell envelope, phospholipids, two-component regulatory systems

Bacillus anthracis is among the few organisms that have been used as a bioterror weapon (1–4). Four infectious syndromes can result from exposure to *B. anthracis* spores: cutaneous, gastrointestinal, inhalation, and injectional anthrax (1, 3, 5–7). Inhalation of anthrax results in the most severe disease, with mortality rates approaching 90% (8). Upon exposure to host tissues, spores are phagocytosed by immune cells in an attempt to eliminate the pathogen. Spores that survive phagocytic attack germinate into vegetative cells that avoid immune-mediated clearance and cause life-threatening disease. Accordingly, *B. anthracis* is well equipped to respond to a range of stressors experienced during vertebrate colonization.

The infectivity of bacteria that colonize mammals, such as *B. anthracis*, is dependent upon the ability to sense and respond to the host environment. Pathogens can rapidly alter gene expression in response to environmental stimuli using two-component systems (TCSs). TCSs typically consist of a membrane-embedded sensor histidine kinase and cognate response regulator. The sensor kinase becomes activated upon exposure to a specific signal(s), resulting in autophosphorylation. The kinase activates the regulator via phosphotransfer, and the regulator, in turn, commonly acts as a transcription factor, resulting in gene expression changes to support survival and growth. Although genes encoding TCSs are often readily identifiable, the activating signals for TCS are not well defined. Some TCSs, such as the TCS PhoPQ, respond to multiple signals. This TCS is conserved between Gram-positive and Gram-negative species and can be activated by antimicrobial peptides or altered metal levels to provide resistance to antimicrobial peptides (9–12). Others, like *Staphylococcus aureus* AgrCA, are activated by binding a single ligand such as the quorum sensing molecule autoinducing peptide (AIP) (13). Disruption of the phospholipid membrane can be sensed by TCSs. For instance, DesKR in *B. subtilis* is a thermosensor that is activated at low temperatures when the cellular membrane condenses to reveal the linker domain in the sensor kinase and promote autokinase activity (14–22). Activation of DesKR results in the synthesis of unsaturated fatty acids that maintain membrane fluidity under colder conditions (14). These are some of the few known examples of TCSs with a defined stimulus and response pattern that is vital for the stability of the cell.

In Gram-positive species, the cell is protected by a single phospholipid bilayer and the peptidoglycan cell wall (23, 24). In some cases, there is an additional proteinaceous S-layer and an antiphagocytic capsule (25–27). Maintenance of an intact cell envelope is required for bacterial survival, including during growth within vertebrates. The bacterial cell envelope provides protection from environmental assaults to maintain redox state, preserve nutrient pools, and defend against antimicrobial attack, among other activities. Targocil is an example of an antibacterial that inhibits elaboration of wall teichoic acid (WTA) in *S. aureus*. Targocil inhibits TarG, the permease component of the ATP binding cassette (ABC) transporter responsible for the export of fully synthesized WTA to the surface of *S. aureus* (28). However, not all Gram-positive pathogens synthesize WTA; one WTA-negative species is *B. anthracis* (29, 30). These findings prompted the hypothesis that targocil activity against *B. anthracis* must occur in a WTA-independent manner.

In this study, we demonstrated that targocil treatment of *B. anthracis* activates a previously unstudied TCS, EdsRS. Upon activation, EdsRS upregulates self-expression and expression of an additional operon, consisting of *BAS1661-BAS1663clsT*. Elevated expression of *clsT* is required for the protection of *B. anthracis* against alterations in barrier permeability caused by targocil treatment, which are heightened in defined media and during spore germination. *clsT* encodes a newly identified cardiolipin synthase that is responsible for increasing the abundance of cardiolipin and thus restoring envelope damage caused by targocil. This work describes how antimicrobial-mediated activation of a two-component system in *B. anthracis* initiates a membrane remodeling response to maintain bacterial fitness.

RESULTS

***Bacillus anthracis* transcriptional responses to the antibacterial compound targocil.** The recently identified antibiotic targocil inhibits WTA biosynthesis in *S. aureus*. To identify the mechanism of action of targocil in *B. anthracis*, which lacks WTA, we defined the transcriptional response of *B. anthracis* to targocil by RNA sequencing. Alterations in the gene expression profile of the parent *B. anthracis* strain after a brief exposure to targocil were measured during mid-exponential-phase growth in rich medium. The attenuated *B. anthracis* Sterne strain (31) served as the parent strain in all experiments in this study. There were 28 total transcripts significantly altered in targocil-treated samples, the majority of which were upregulated (Fig. 1A; see also Table S1, Table S2, Table S3, and Table S4 in the supplemental material). The primary pathways affected by targocil included transport and gene regulation, though transcriptional changes were also observed in genes involved in metabolism and electron transport and in phage genes (Fig. 1B). One set of genes, *BAS5200* to *BAS5203*, displayed the highest fold change compared to untreated cells. Alignment of the sequencing reads to the genome suggests that genes *BAS5200* to *BAS5203* are in an operon and are expressed as a monocistronic transcript. This operon codes for a putative response regulator (*BAS5200*), a histidine kinase (*BAS5201*), an ABC transporter permease (*BAS5202*), and an ABC transporter ATP-binding protein (*BAS5203*). BAS5200 and BAS5201 contain domains associated with known two-component systems. BAS5201 is predicted to contain a HisKA3 phosphoacceptor domain and a HATPase domain for ATP hydrolysis (32, 33). BAS5200 contains a phosphoacceptor domain for activation by the histidine kinase and a GerE helix-turn-helix domain for DNA binding (34). *BAS5202-BAS5203* codes for a putative ABC transporter. This family of proteins is associated with the transport of a wide range of substrates, including antimicrobials (35). Due to the described role of targocil in disrupting barrier function, and for reasons described below, we named this operon the <u>e</u>nvelope <u>d</u>isruption <u>s</u>ensor (*eds*) system (*edsRSAB*) (Fig. 1C). Quantitative reverse transcription-PCR (qRT-PCR) was performed on transcripts isolated from targocil-treated samples to confirm RNA sequencing results. Treatment of the parent strain with targocil showed levels of expression of both *edsR* and *edsS* that were higher than those seen with untreated samples (Fig. 1D). Collectively, the findings suggest that targocil treatment induces expression of a putative TCS (*edsRS*) and an ABC transporter (*edsAB*).

EdsRS signaling is activated in response to targocil. Targocil at high concentrations is toxic to *B. anthracis* grown in rich media (Fig. 2A). However, the resistance of *B. anthracis* to targocil is over 100-fold higher than the level previously observed in *S. aureus* (36). We hypothesized that the EdsRS two-component system is activated in *B. anthracis* to resist targocil-dependent killing. This was quantified using a vector that contained the *eds* promoter driving expression of a catechol oxidase, XylE. Activation of the promoter can be measured by quantifying the rate of conversion of catechol to a colorimetric product using a spectrophotometer (37). In the parent strain, targocil treatment increased P_{eds} activation compared to a vehicle control (Fig. 2B). The $\Delta edsRS$ mutant lacks this activation, and this phenotype can be complemented by expressing *edsRS* in *trans* ($\Delta edsRS$ *BAS5207::edsRS*) (Fig. 2B). These results demonstrate that targocil exposure activates *edsRSAB* expression and that this is dependent on EdsRS. However, when the parent strain and $\Delta edsRS$ were grown in rich medium containing increasing concentrations of targocil, increased susceptibility of $\Delta edsRS$ to targocil was not observed (Fig. 2). These data suggest that targocil-dependent activation of EdsRS signaling induces expression of its own operon, but that this TCS-activation is not required for resistance to toxicity. We propose that this could be due to the presence of additional mechanisms that can defend against targocil-induced damage and are active in mid-log cultures. EdsRS is activated under these conditions, but alternative systems could compensate in maintenance of cellular stability.

Targocil activates EdsRS-dependent expression of *BAS1661-BAS1663clsT*. To define the regulon of EdsRS, we performed RNA sequencing on the parent strain and
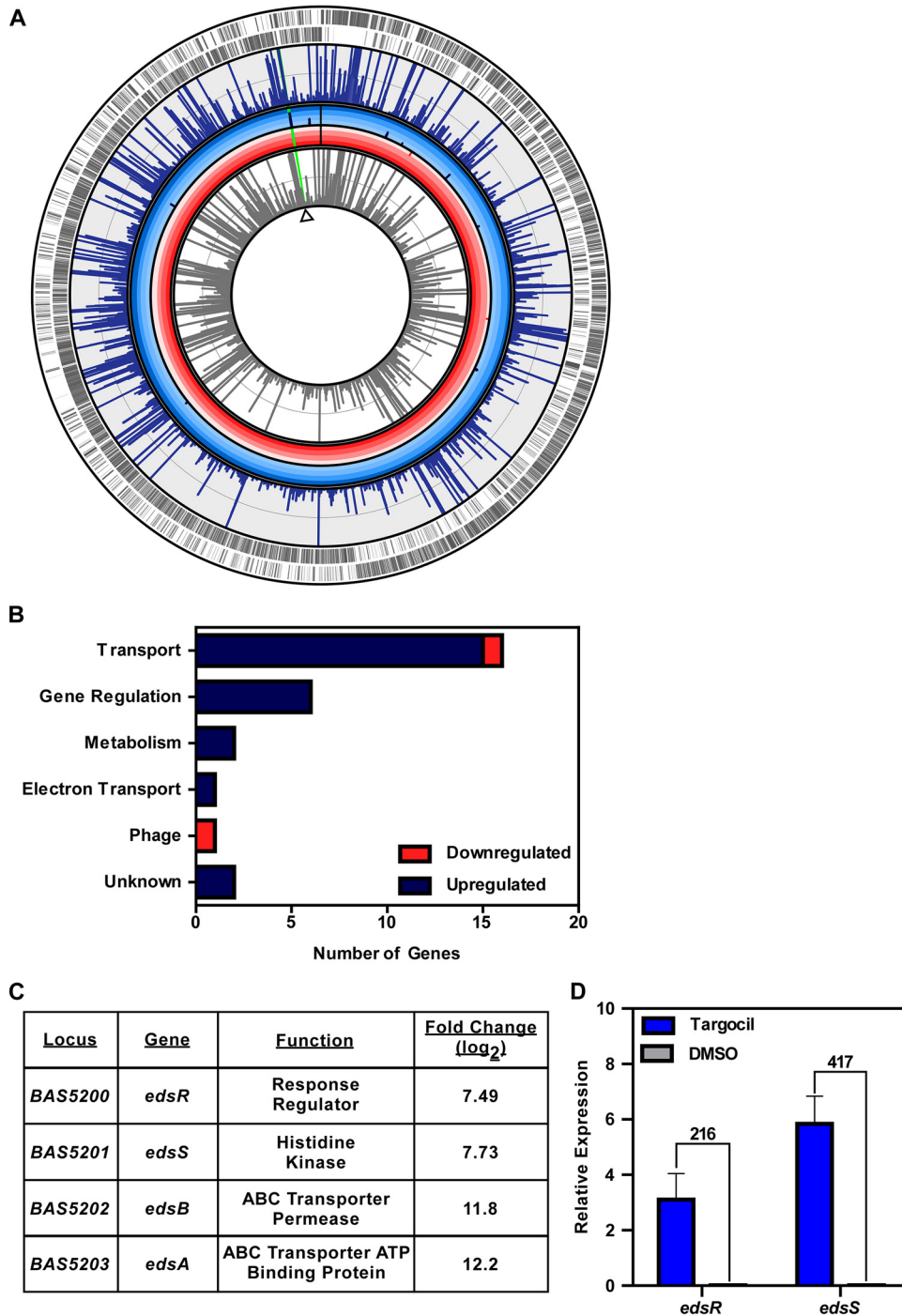
FIG 1 Targocil induces gene expression changes in *B. anthracis*. (A) Genomic map of *B. anthracis* Sterne. Indicated are the open reading frames (outer ring in gray) and on which strand the gene is present. The degree of expression for each transcript is shown for cultures grown in targocil (blue bars in outer ring) and DMSO control (gray bars). Those transcripts which were significantly altered with a $\log_2$ fold change value of at least 2 and the degree of fold change in increments of 3 (concentric gradient) are shown for transcripts that were upregulated (navy bars) and downregulated (red bars). The most significantly upregulated operon is indicated (green bar). (B) The number of transcripts that fall into unique KEGG pathways are displayed, as well as whether they were upregulated or downregulated. (C) Fold change values for those transcripts that were most significantly increased in abundance after targocil treatment. Included are the locus, gene name, predicted protein function, and $\log_2$ fold change. (D) qRT-PCR validation of transcriptome sequencing (RNA-Seq) results for the *edsRS* operon represented by targocil-induced expression relative to expression in DMSO. Fold changes between targocil-treated and DMSO-treated samples are shown above the relative expression bars. Data represent averages of results from three independent experiments performed in biological triplicate ± standard errors of the means (SEM).
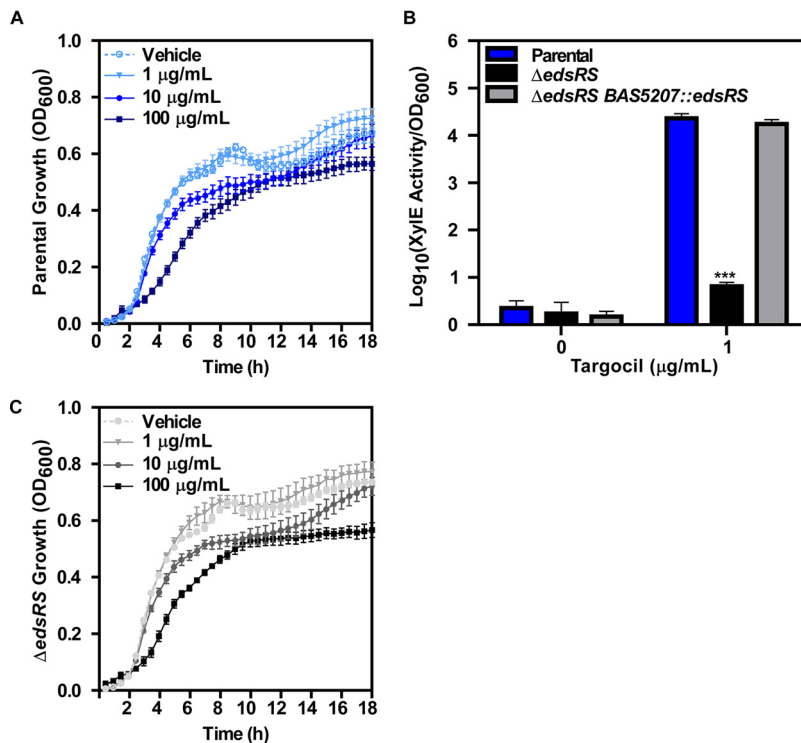
FIG 2 Targocil induces expression of *edsRSAB* in an EdsRS-dependent manner. (A) Growth of *B. anthracis* Sterne (parental strain) measured by optical density at 600 nm (OD_{600}) in LB containing 0, 1, 10, or 100 μg/ml targocil. Data represent averages of results from two independent experiments performed in biological triplicate $\pm$ SEM. (B) Activity of *eds* promoter in response to targocil was quantified using parental, $\Delta edsRS$, and $\Delta edsRS$ BAS5207::*edsRS* strains carrying the *xylE* reporter plasmid. Strains were grown in triplicate in the presence of vehicle or 1 μg/ml of targocil for 6 h. XylE activity was quantified and normalized to bacterial density at the time of assay termination. Data represent averages of results from three independent experiments performed in biological triplicate $\pm$ SEM. Statistical significance compared to parental strain results was determined using a two-way analysis of variance (ANOVA) with a Tukey's test adjustment for multiple comparisons (***, $P \leq 0.001$). (C) Growth of the $\Delta edsRS$ strain measured by OD_{600} in LB containing 0, 1, 10, or 100 μg/ml targocil. Data represent averages of results from two independent experiments performed in biological triplicate $\pm$ SEM.

the $\Delta edsRS$ mutant, which were treated with or without targocil. Targocil and EdsRS are required for expression changes of *edsRSAB* and of an uncharacterized operon, *BAS1661* to *BAS1664*. Both operons were upregulated in the presence of targocil, in an EdsRS-dependent manner (Fig. 3A). Alignment of the RNA sequencing reads to the region of *BAS1661* to *BAS1664* suggests that these genes are expressed as an operon. This operon contains putative ABC transporter genes (*BAS1661-BAS1663*) and a putative cardiolipin synthase gene (*BAS1664*) (Fig. 3B). BAS1661-BAS1663 are predicted to contain domains from the ABC-2 subfamily of transporters associated with the export of drugs and carbohydrates (38). In addition to *BAS1664*, the genome of *B. anthracis* Sterne includes four other putative cardiolipin synthase genes (see Fig. S1A in the supplemental material). BAS1664 contains the HKD motif associated with this superfamily of proteins that is required for the synthesis of cardiolipin (39, 40). There is significant protein identity shared between the previously described ClsA and ClsB proteins of *B. subtilis* and BAS1112 and BAS5195, respectively, but BAS1664 shares less identity with the previously characterized proteins (Fig. S1B). On the basis of the activation in response to targocil, we have named *BAS1664* <u>c</u>ardio<u>l</u>ipin <u>s</u>ynthase <u>t</u>argocil (*clsT*). To confirm that EdsRS activation results in upregulation of *BAS1661-BAS1663clsT*, we performed qRT-PCR on RNA extracted from the parent strain and the $\Delta edsRS$ mutant, either treated with targocil or left untreated (Fig. 3C). These results indicate that targocil activates EdsRS to increase expression of *BAS1661-BAS1663clsT*. This suggests that ClsT is a previously unstudied cardiolipin synthase that is expressed when EdsRS is activated by targocil.
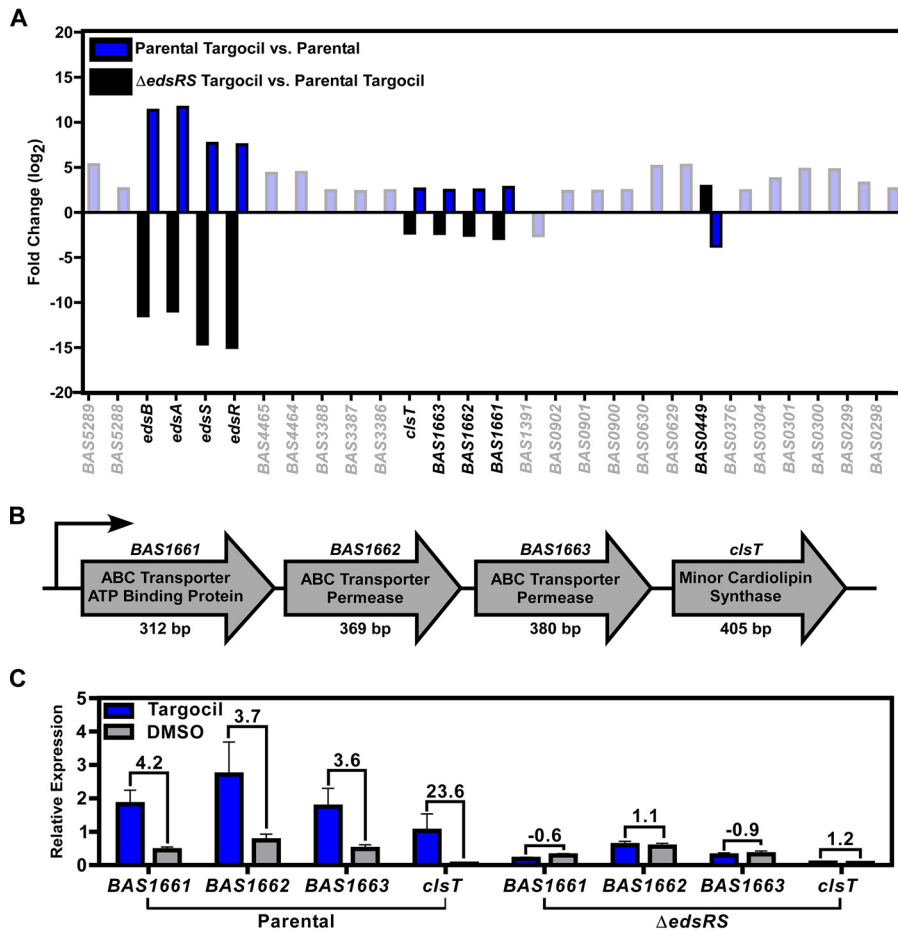
FIG 3 Targocil activation of EdsRS leads to induction of *BAS1661-BAS1664* expression. (A) Depiction of the significant fold changes for two distinct RNA sequencing comparisons. Shown are those genes altered in *B. anthracis* Sterne (parental) treated with targocil compared to the parental strain left untreated (blue) and the Δ*edsRS* mutant treated with targocil compared to the parental strain treated with targocil (black). Data for transcripts shown as having been altered under the same conditions but in the opposite direction indicate genes altered by targocil that require *edsRS* (dark bars). (B) *BAS1661* to *BAS1663clsT* encode an ABC transporter ATP binding protein (*BAS1661*), an ABC transporter permease (*BAS1662*), an ABC transporter permease (*BAS1663*), and a cardiolipin synthase (*clsT*). (C) qRT-PCR validation represented by relative levels of expression of the *BAS1661-BAS1663clsT* operon in the parental strain and a Δ*edsRS* mutant under conditions of growth in DMSO and targocil. Data represent averages of results from three independent experiments performed in biological triplicate ± SEM. Fold changes between targocil-treated and DMSO-treated samples are shown above the relative expression bars.

EdsRS signaling is required for spore outgrowth in the presence of targocil. Targocil exposure inhibits growth of *B. anthracis*. On the basis of the EdsRS-dependent activation of ClsT, we hypothesized that EdsRS senses targocil to coordinate the increase in barrier stability required for growth during treatment. To test this hypothesis under defined conditions, growth experiments were performed in RPMI medium with Casamino Acids (41–44). Growth of the parent strain during targocil treatment in RPMI medium was assessed by measuring optical density at 600 nm (OD_{600}) over time. Cultures grown in 100 μg/ml targocil did not reach the same maximum optical density as those grown in the presence of vehicle control, indicating that targocil is toxic in this semidefined media (Fig. 4A).

The infectious particle of *B. anthracis* is the endospore, which germinates during infection of a mammalian host (1, 3, 45–48). As a spore germinates, the cell must elongate into a full-length vegetative cell. This process involves the elaboration of cellular barriers, including the phospholipid bilayer, S-layer, and peptidoglycan wall. We hypothesized that targocil would be more toxic to newly germinating *B. anthracis*
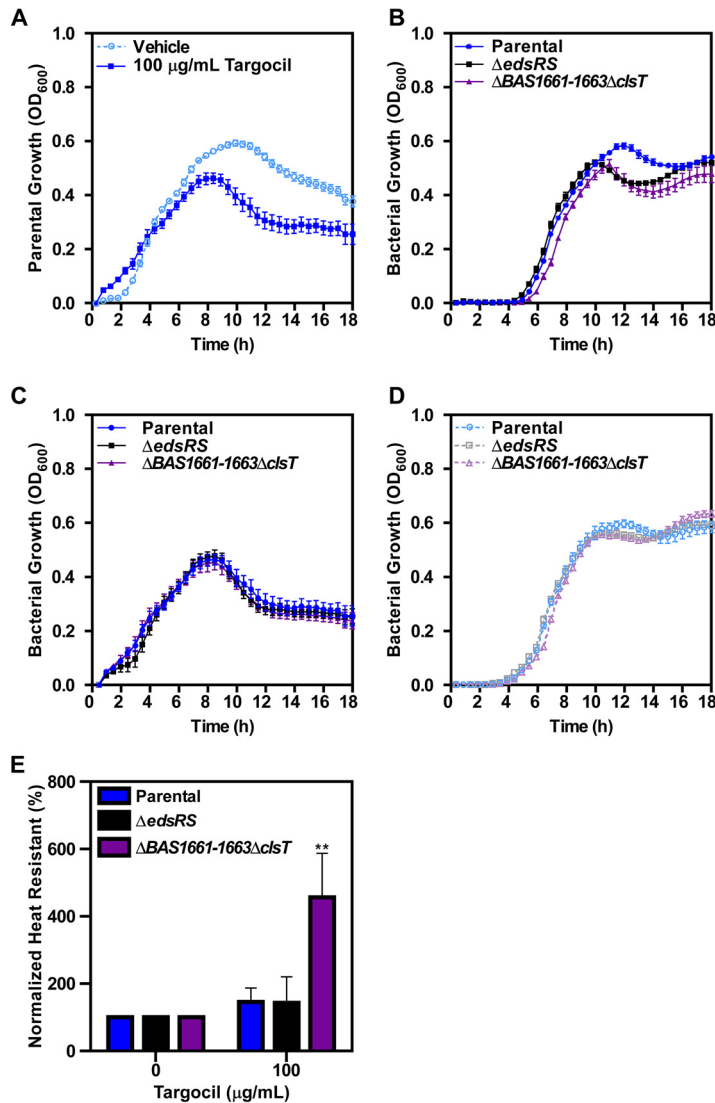
FIG 4 Activation of EdsRS signaling is required for spore germination during targocil treatment in defined media. (A) Growth of *B. anthracis* Sterne (parental strain) measured by OD_{600} in RPMI medium plus 1% Casamino Acids containing 0 or 100 μg/ml targocil. Data represent averages of results from three independent experiments performed in biological quadruplicate $\pm$ SEM. (B) Germination and subsequent growth of parental strain, $\Delta edsRS$ mutant, and $\Delta BAS1661$-$BAS1663\Delta clsT$ mutant spores in RPMI medium plus 1% Casamino Acids containing 25 μg/ml targocil. Data represent averages of results from three independent experiments performed in biological triplicate $\pm$ SEM. (C) Growth of the parental, $\Delta edsRS$, and $\Delta BAS1661$-$BAS1663\Delta clsT$ strains measured by OD_{600} in RPMI medium plus 1% Casamino Acids containing 100 μg/ml targocil. Data represent averages of results from three independent experiments performed in biological quadruplicate $\pm$ SEM. (D) Germination and subsequent growth of the parental, $\Delta edsRS$, and $\Delta BAS1661$-$BAS1663\Delta clsT$ spores in RPMI medium plus 1% Casamino Acids containing a vehicle control. Data represent averages of results from three independent experiments performed in biological triplicate $\pm$ SEM. (E) After 5 min of incubation of the parental, $\Delta edsRS$, and $\Delta BAS1661$-$BAS1663\Delta clsT$ spores with rich media with and without 100 μg/ml targocil, samples were analyzed for total bacterial counts and heat resistance. The percentage of heat-resistant bacteria is normalized to the control treated sample. Data presented are the averages of three independent experiments performed in biological triplicate $\pm$ SEM. Statistical significance compared to other treated samples was determined using a two-way ANOVA with a Tukey's test adjustment for multiple comparisons (**, $P \leq 0.01$).

spores than to actively growing vegetative cells. To test this, complete growth kinetics after spores were inoculated into RPMI medium containing targocil were assessed. Outgrowth of spores lacking $\Delta BAS1661$-$BAS1663\Delta clsT$ showed a slight growth delay compared to the parental spores in the presence of targocil (Fig. 4B). Additionally, both the $\Delta BAS1661$-$BAS1663\Delta clsT$ spores and the $\Delta edsRS$ spores exhibited altered growth

kinetics at later time points in stationary phase upon targocil exposure. These phenotypes were not observed when exponential-phase cultures were used for inoculation to determine growth curves under the same conditions (Fig. 4C). The mutant strains did not display altered growth compared to the parental strain in semidefined medium containing a vehicle control (Fig. 4D). This indicates that the Δ*BAS1661-BAS1663*Δ*clsT* spores and the Δ*edsRS* spores were not less fit overall and that the altered growth was due to the activity of targocil. We hypothesized that the defect in outgrowth observed in the Δ*BAS1661-BAS1663*Δ*clsT* spores and the Δ*edsRS* spores (Fig. 4B) was due to delayed spore germination in the presence of targocil. An indicator of spore germination is the loss of heat resistance. The degree of heat resistance that remained in samples exposed to rich media in the presence of vehicle or targocil was measured. Germination of the Δ*BAS1661-BAS1663*Δ*clsT* strain was significantly reduced in samples treated with targocil compared to all other conditions (Fig. 4E). Disc diffusion assays were performed using the parent strain and the Δ*edsRS* and Δ*BAS1661-BAS1663*Δ*clsT* strains challenged with a panel of toxic compounds. Of those tested, no additional compounds were found to have differential toxicity in the mutant strains compared to the parent strain (Fig. S2). Therefore, EdsRS, BAS1661-BAS1663, and ClsT are important for protecting against targocil during spore germination.

EdsRS activation of *clsT* expression is required to combat targocil-induced envelope permeability. ClsT is predicted to be a cardiolipin synthase. Cardiolipin is a component of phospholipid bilayers and is primarily associated with bacterial and mitochondrial membranes. Cardiolipin makes up roughly 17% of total phospholipid in pathogenic bacillus species and is mobilized as a component of the membrane damage response (49, 50). Due to the increased targocil sensitivity of the Δ*BAS1661-BAS1663*Δ*clsT* mutant during spore germination and outgrowth, upregulation of *clsT* in targocil treatment, and the role of cardiolipin in membrane maintenance, we hypothesized that targocil induces barrier damage in *B. anthracis*. The permeability of the cellular envelope can be quantified using an ethidium bromide (EtBr) uptake assay to measure the rate at which EtBr crosses the cell wall and lipid bilayer (51–53). Targocil induced permeability in the parent *B. anthracis* strain in both LB and RPMI medium plus Casamino Acids (Fig. 5A). However, the rate of EtBr uptake after targocil treatment was significantly higher in the cultures grown in semidefined media than in those grown in rich media (Fig. 5B). From these results, we conclude that targocil increases cellular permeability.

Next, we hypothesized that activation of expression of *BAS1661-BAS1663clsT* by EdsRS is required for the response to targocil-induced envelope damage. In the EtBr uptake assay, the Δ*BAS1661-BAS1663*Δ*clsT* and Δ*edsRS* strains exhibited increased barrier permeability relative to the parent strain after 30 min of exposure to 100 μg/ml targocil in RPMI medium (Fig. 5C). Constitutive expression of *edsRS* in the Δ*edsRS* background resulted in a significant decrease in the permeability of this mutant, reaching levels comparable to those seen with the parent strain (Fig. 5D). This indicates that EdsRS activation is important to protect against targocil-induced envelope permeability but does not exclude the possibility that activation occurs via direct interaction of targocil with EdsS in the membrane. Interestingly, the increased permeability of the Δ*BAS1661-BAS1663*Δ*clsT* strain was able to be complemented by expression in *trans* of the cardiolipin synthase gene *clsT*. In fact, overexpression of *clsT* led to a 35% reduction in envelope permeability compared to the Δ*BAS1661-BAS1663*Δ*clsT* strain in the presence of targocil (Fig. 5D). These results indicate that *edsRS* and *clsT* are required for preserving envelope integrity following targocil exposure.

The addition of exogenous cardiolipin to bacteria can alter the phenotypes observed with envelope-targeting antimicrobials (54–56). Therefore, cardiolipin was added to targocil-exposed Δ*BAS1661-BAS1663*Δ*clsT* cultures, which resulted in significantly reduced envelope permeability (Fig. 5E). The rates of EtBr uptake in the vehicle and cardiolipin-only control samples were comparable (Fig. 5F), suggesting that the effect of exogenous cardiolipin is realized only upon membrane damage. Overall, these
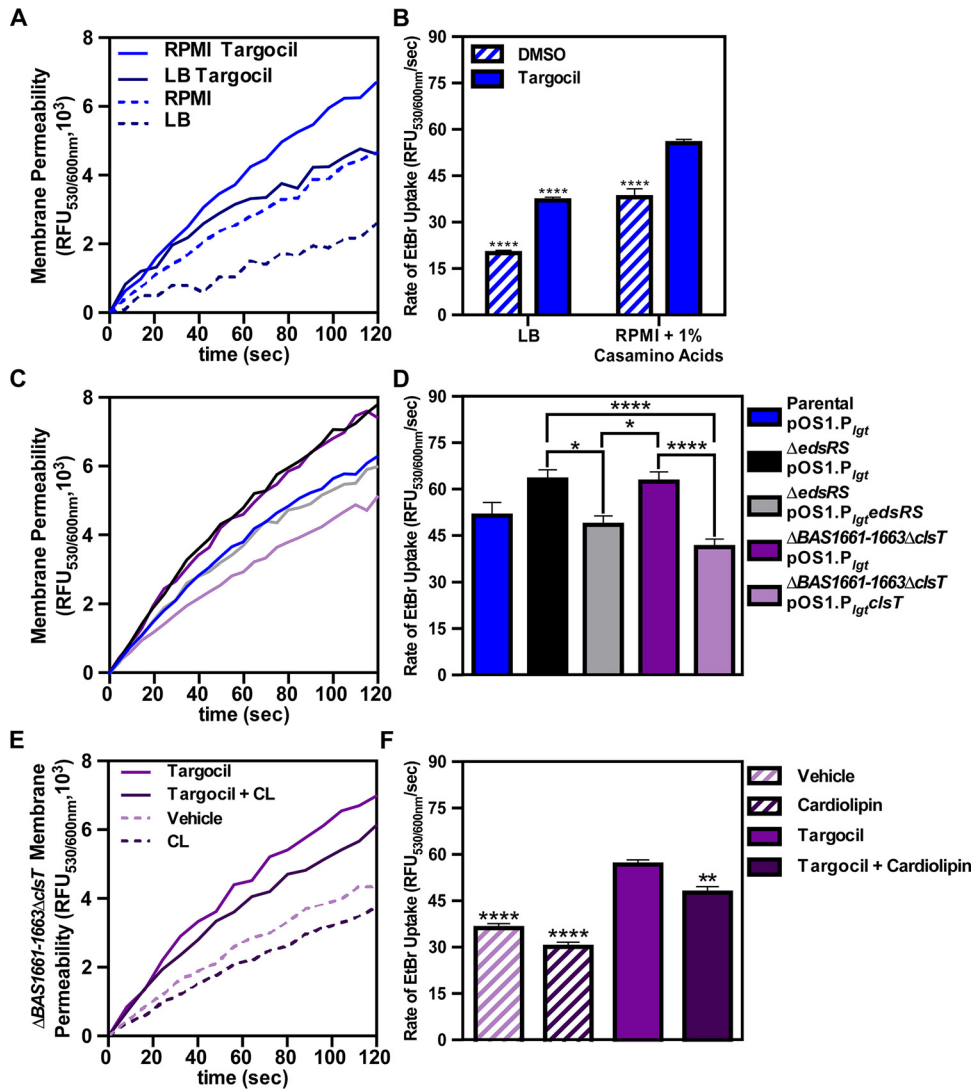
FIG 5 Cardiolipin synthesis is required for an intact cellular barrier during targocil treatment. (A) Ethidium bromide uptake over time after growth of *B. anthracis* Sterne (parental strain) in RPMI medium plus 1% Casamino Acids or LB with or without 100 μg/ml targocil. Data represent averages of results from three independent experiments performed in biological triplicate ± SEM. (B) The rate of ethidium bromide uptake shown in panel A. Data represent averages of results from three independent experiments performed in biological triplicate ± SEM. Statistical significance compared to parental strain was determined using a two-way ANOVA with a Tukey's test adjustment for multiple comparisons (****, $P \le 0.0001$). (C) Ethidium bromide uptake over time after growth of the parental strain, Δ*edsRS* strain, and Δ*BAS1661–BAS1663*Δ*clsT* strain containing either empty vector (pOS1 P$_{lgt}$) or vectors for phenotypic complementation in RPMI medium plus 1% Casamino Acids with 100 μg/ml targocil. Data represent averages of results from three independent experiments performed in biological triplicate ± SEM. (B) The rate of ethidium bromide uptake shown in panel C. Data represent averages of results from three independent experiments performed in biological triplicate ± SEM. Statistical significance compared to the parental strain was determined using a one-way ANOVA with a Tukey's test adjustment for multiple comparisons (*, $P \le 0.05$; ****, $P \le 0.0001$). (E) Ethidium bromide uptake over time after growth of strain Δ*BAS1661–BAS1663*Δ*clsT* in RPMI medium plus 1% Casamino Acids with or without 100 μg/ml targocil, in the presence and absence of 100 μg/ml cardiolipin (CL). Data represent averages of results from three independent experiments performed in biological quadruplicate ± SEM. (F) The rate of ethidium bromide uptake shown in panel E. Data represent averages of results from three independent experiments performed in biological quadruplicate ± SEM. Statistical significance compared to targocil-treated samples was determined using a one-way ANOVA with a Dunnett's test adjustment for multiple comparisons (**, $P \le 0.01$; ****, $P \le 0.0001$).

data indicate that EdsRS and ClsT respond to targocil-mediated envelope damage in *B. anthracis*.

EdsRS responds to targocil-induced envelope permeability via synthesis of cardiolipin. EdsRS responds to targocil and increases expression of *clsT*, and this
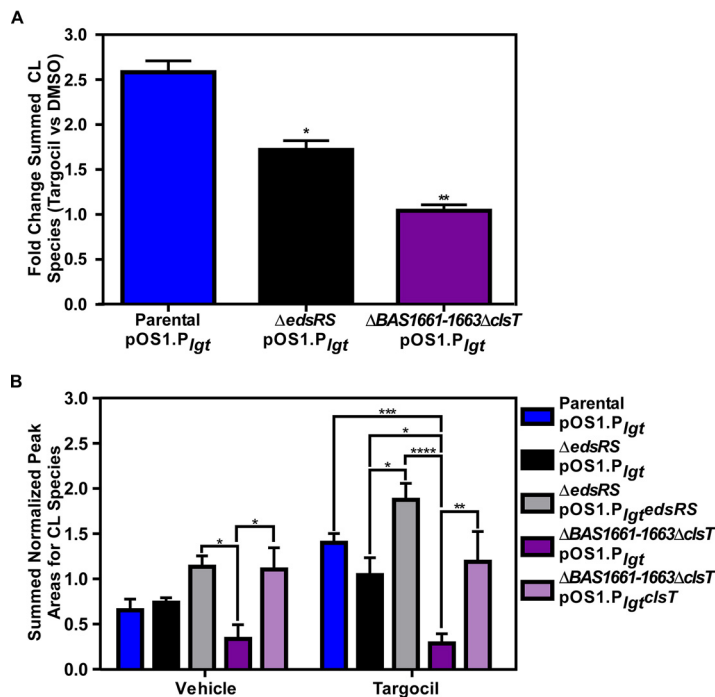
FIG 6 Targocil activation of EdsRS is required for ClsT-dependent increases in cardiolipin. (A) Whole-cell cardiolipin relative quantification using liquid chromatography coupled to tandem mass spectrometry (LC-MS/MS). Fold change of *B. anthracis* Sterne (parental strain), ΔedsRS, and ΔBAS1661-BAS1663ΔclsT strains grown in RPMI medium plus 1% Casamino Acids and then exposed to 100 μg/ml targocil was determined relative to vehicle-treated samples. Data represent averages of results from two technical runs performed in biological triplicate ± SEM. Statistical significance of results of comparisons of samples between treatment groups was determined using a two-way ANOVA with a Tukey's test adjustment for multiple comparisons (*, $P \leq 0.05$; **, $P \leq 0.01$). (B) Cardiolipin relative quantification of complementation strains for the parental, ΔedsRS, and ΔBAS1661–BAS1663ΔclsT strains using LC-MS/MS. Cultures were also grown in RPMI medium plus 1% Casamino Acids and then exposed to 100 μg/ml targocil for 30 min. Data represent averages of results from two technical runs performed in biological triplicate ± SEM. Statistical significance compared to targocil-treated samples was determined using a two-way ANOVA with a Tukey's test adjustment for multiple comparisons (*, $P \leq 0.05$; **, $P \leq 0.01$; ***, $P \leq 0.001$; ****, $P \leq 0.0001$).

activation maintains the cell barrier in *B. anthracis*. Therefore, we hypothesized that cardiolipin levels within the bacterial membrane increase in the presence of targocil and that this is dependent on expression of both *edsRS* and *clsT*. To test this, liquid chromatography with tandem mass spectrometry (LC-MS/MS) was used to quantify relative levels of cardiolipin species in *B. anthracis*. Whole-cell lysates were collected after a 30-min exposure to 100 μg/ml targocil in RPMI medium plus Casamino Acids prior to lipid extraction and LC-MS/MS analysis (Fig. S3). Comparisons of cardiolipin levels in the parent strain with and without targocil exposure indicated that there was a significant increase in the level of cardiolipin after treatment (Fig. 6A). In support of this hypothesis, the ΔedsRS and ΔBAS1661-BAS1663ΔclsT strains did not show a significant increase in cardiolipin levels upon targocil treatment (Fig. 6A). In accordance with the idea of the importance of ClsT, the ΔBAS1661-BAS1663ΔclsT strain had a lower level of cardiolipin than the parent strain even in the absence of targocil. The phenotypes observed for the mutant strains were complemented above the parent strain levels when *edsRS* or *clsT* was constitutively expressed in *trans* (Fig. 6B). Consistent with earlier experiments (Fig. 5C and D), complementation of cardiolipin levels in the ΔBAS1661-BAS1663ΔclsT strain required only expression of the cardiolipin synthase (*clsT*). Therefore, the cellular response to targocil involves the synthesis of cardiolipin by ClsT. The expression of *clsT* under these conditions is driven by signaling through EdsRS, establishing this TCS as being required for sensing and responding to targocil-mediated envelope damage in *B. anthracis*.

DISCUSSION

In this study, the *B. anthracis* response to the antimicrobial compound targocil was analyzed. Targocil induces damage to the cellular envelope (Fig. 5A and B) and activates the TCS EdsRS (Fig. 2B). Upon activation, EdsRS increases expression of a cardiolipin synthase (ClsT) (Fig. 3C). EdsRS and ClsT are required for the production of cardiolipin in response to targocil (Fig. 6) to protect *B. anthracis* from damage caused by targocil (Fig. 5C to E). Collectively, these data uncover a TCS that is activated to alter membrane composition in response to cell envelope damage.

Due to the synthetic nature of targocil, it is unlikely that EdsRS evolved to respond to this antimicrobial. However, the ability of *B. anthracis* to activate a TCS in response to envelope damage highlights the adaptability of this pathogen. The presence of over 40 TCSs equips *B. anthracis* to respond to a wide range of environments (57). Thus far, studies have assigned activating stimuli to 11 of these systems, but not all of them have defined downstream functions within the cell (58–64). Despite the importance of TCSs, there are still over 30 histidine kinase-response regulator pairs in *B. anthracis* that are not well understood. Our work exemplifies the importance of studying TCSs in this pathogen to uncover the contribution of signaling responses to anthrax pathogenesis.

The data presented here suggest that cardiolipin abundance in the membrane affects the efficacy of antimicrobials targeted to the cell envelope and that alterations in the regulation of cardiolipin synthesis represent a bacterial strategy for adaptation. *B. anthracis* encodes five cardiolipin synthase genes. This genetic redundancy in the biogenesis of cardiolipin has been reported for other bacterial species. Bacterial cardiolipin synthases (Cls) classically synthesize cardiolipin through the condensation of two molecules of phosphatidylglycerol to produce cardiolipin and glycerol (55, 65). The *cls* genes have been studied in *Escherichia coli*, which codes for three of these enzymes (ClsA, ClsB, and ClsC). Each of the Cls enzymes in this bacterium uses unique precursors and contributes to cardiolipin abundance under distinct conditions, including stationary or hyperosmotic growth (40, 66). This enables tight control of membrane phospholipid composition and preservation of resources. Similarly to *E. coli*, *B. subtilis* encodes three cardiolipin synthases (ClsA, YwjE, and YwiE) with differentially ascribed functions (67). ClsA is the primary cardiolipin synthase in this species during vegetative growth and osmotic stress but works together with YwjE to produce the phospholipid during the process of sporulation (67–69). Although it has not been empirically tested, transcription data suggest that the third synthase gene, *ywiE*, is involved in the response to heat shock (70).The use of multiple Cls variants is important in Gram-positive pathogens. The human pathogen *S. aureus* expresses two cardiolipin synthases (Cls1 and Cls2) (71, 72). Cls2 is the primary producer of cardiolipin, which accumulates in *S. aureus* during stationary-phase growth. However, after phagocytosis and during growth under high-salt conditions, both Cls1 and Cls2 contribute to cardiolipin synthesis (72). These examples highlight the versatility of bacterial phospholipid synthesis. Synthesis of cardiolipin depends on the growth phase and specific stress encountered and results in unique routes of biogenesis depending on available lipid resources. The extreme adaptability of *B. anthracis* to survive in the environment and during infection of mammalian hosts is likely supported not only by the presence of TCSs but also by flexibility in the pathways used for generation of key cellular molecules such as cardiolipin.

Cardiolipin has been associated with the efficacy of antimicrobials, specifically, daptomycin. Daptomycin forms pores in the membranes of bacteria, resulting in barrier permeabilization, and has been linked to disruption of cell division (73–75). Daptomycin was first used clinically in 2003, and since then, resistance to this drug has been reported in *Enterococcus* and *Staphylococcus* species (76). Sequencing of daptomycin-resistant *Enterococcus* strains identified mutations within a cardiolipin synthase (77, 78). Although the mechanism by which cardiolipin protects against daptomycin remains unclear, a follow-up study found that addition of exogenous cardiolipin to liposomes diminished the pore-forming activity of daptomycin (55). However, a transposon

insertion sequencing (Tn-Seq) study in *S. aureus* found that mutation of a cardiolipin synthase conferred resistance to daptomycin (79). These results suggests that bacterial cells can increase the abundance of cardiolipin within their outer membranes to repair damage by antimicrobials that breach this barrier, similarly to the findings presented here in *B. anthracis*, but that the consequence of these modifications can be species specific.

While cardiolipin synthesis can enable bacteria to resist some antimicrobial compounds, the role of cardiolipin in the response to antimicrobials is context dependent. Cardiolipins can also increase the efficacy of other antimicrobials. For instance, the toxicity of an amphiphilic aminoglycoside derivative against *Pseudomonas aeruginosa* was enhanced with addition of cardiolipin to the culture conditions (56). The derivative altered the biophysical structure of lipid bilayers to cause increased permeability in a cardiolipin-dependent manner (80). In another example, the activity of plantazolicin was interrogated in *B. anthracis* (54). Plantazolicin inserts into the cellular envelope of bacilli and disrupts membrane potential, indicating damage to the bilayer. Of the species tested, *B. anthracis* was the only Gram-positive organism sensitive to this compound (81). That study observed that EdsRS (then referred to as BAS5200-BAS5201) was upregulated upon plantazolicin exposure, providing an additional link between EdsRS and damage to the envelope of *B. anthracis* (54). In an effort to understand the mechanism of plantazolicin toxicity, selection studies were performed looking for resistant mutants. Molohon et al. identified isolates that showed resistance phenotypes containing mutations within *BAS1662* and *BAS1663* and the promoter region of the *BAS1661-BAS1663clsT* operon. As a follow-up to this finding, they showed that the presence of exogenous cardiolipin increases the efficacy and membrane insertion of plantazolicin. Therefore, EdsRS is activated by treatment with plantazolicin; however, subsequent induction of *BAS1661-BAS1663clsT* and increase in cardiolipin levels are detrimental due to the mechanism of drug insertion. Using two small molecules that are similar in function but divergent in mechanism, the work of Molohon et al. and the results reported here support the idea of links between envelope disruption, EdsRS two-component system signaling, and cardiolipin synthesis.

The intracellular environment of host immune cells is a site for germination of *B. anthracis* spores during infection (82–87). The importance of EdsRS signaling to the germination and viability of *B. anthracis* during outgrowth in the presence of envelope-damaging agents indicates that this system could be used during dissemination in vertebrate hosts. TCSs are important for intracellular survival, where they enable a response to metal limitation or acidic environments (88, 89). Future studies are needed to test the role of EdsRS signaling in resistance to barrier attack and germination within phagocytes. The subsequent EdsRS-dependent induction of ClsT synthesis of cardiolipin may reverse barrier permeability to promote survival of bacilli (Fig. 3C, 4B, 5C to F, and 6). Cardiolipin synthesis is induced after phagocytosis occurs in *S. aureus* (72). The kinetics of this induction in *S. aureus* suggest that increased membrane cardiolipin levels are important for defense against later stages of immune attack following escape from the host phagocyte (72). Therefore, the bacteria may respond to recognition of the host environment to prepare for survival during infection. The precise role of cardiolipin synthesis in *B. anthracis* immune evasion should be elucidated in future studies as this suggests a role for EdsRS in defense against host attack. Reacting to host effectors in this manner may promote *B. anthracis* pathogenesis, providing significant insight into how this organism causes severe infections.

MATERIALS AND METHODS

Bacterial strains and growth conditions. The bacterial strains (Table 1), plasmids (Table 2), and primers (Table 3) used in this study are listed in the indicated tables. *Bacillus anthracis* strain Sterne was used in all experiments under biosafety level 2 (BSL2) conditions (31). Cultures were streaked from glycerol freezer stocks on LB agar (LBA) plates and grown at 30°C for 16 h. LB was inoculated using a single colony from these plates. Cultures were grown at 30°C with shaking at 180 rpm and aeration for all overnight growth or for any period of growth over 8 h. For growth assays performed for 8 h or less, growth occurred at 37°C. As noted, experiments were performed in RPMI medium (Thermo Fisher Scientific) plus 1% (wt/vol) Casamino Acids to serve as a defined medium. Plasmids were constructed

TABLE 1 Bacterial strains

Species	Genotype	Description	Reference(s) or source
B. anthracis strain Sterne	Wild type/parental	Wild-type/parental laboratory stock	31
B. anthracis strain Sterne	Δ*edsRS*	In-frame deletion of *BAS5200* and *BAS5201*	This study
B. anthracis strain Sterne	Δ*edsRS BAS5207::edsRS*	In-frame deletion of *BAS5200* and *BAS5201* and genomic complementation of *BAS5200* and *BAS5201* within *BAS5207*	This study
B. anthracis strain Sterne	Δ*BAS1661-BAS1663*Δ*clsT*	In-frame deletion of *BAS1661, BAS1662, BAS1663,* and *clsT*	This study
E. coli strain K1077	Wild type	Wild-type laboratory stock for cloning	90
S. aureus strain RN4220	Wild type	Wild-type laboratory stock for cloning	101, 102

using *E. coli* DH5α or TOP10 strains. Plasmids were then moved from *E. coli* to *B. anthracis* after first transforming them into *E. coli* K1077 or *S. aureus* RN4220. Antibiotics concentrations used were carbenicillin at 50 μg/ml for *E. coli* (reporter and complementation vectors), chloramphenicol at 10 μg/ml for *S. aureus* and *B. anthracis* (reporter and complementation vectors), and kanamycin at 20 μg/ml in *B. anthracis* and 40 μg/ml in *E. coli* (genetic manipulation vector).

Preparation of compound stocks. Carbenicillin stocks (50 mg/ml) were prepared in H_2O and stored at −20°C. Chloramphenicol stocks (10 mg/ml) were made in 70% EtOH and stored at −20°C. Targocil stocks (10 mg/ml) were made in dimethyl sulfoxide (DMSO) and stored at −20°C. A stock of cardiolipin sodium salt (10 mg/ml) was made in 100% EtOH and stored at −20°C. All chemicals were purchased from Sigma-Aldrich unless otherwise noted.

Genetic manipulation of *B. anthracis*. Genetic manipulation was performed as previously described (58, 59). Electroporations were performed with modifications as described previously (58, 59, 90). The generation of knockout strains was performed by inserting the flanking sequences for genes of interest in the mutagenesis plasmid pLM4. Briefly, flanking sequences were amplified using a distal primer containing a restriction enzyme site and a proximal primer containing a short sequence overlapping the adjacent flanking region. PCR-amplified DNA was fused using PCR sequence overlap extension (PCR-SOE) as described previously (91). *BAS5207* was selected as a *B. anthracis* strain Sterne pseudogene based on NCBI RefSeq annotation (GenBank genomic sequence accession no. NC_005945). In other strains, including *B. cereus* ATCC 14597 and *B. thuringiensis* BMB181, *BAS5207* orthologues are annotated as encoding predicted LPXTG cell wall anchor domain-containing proteins with homology to collagen adhesion proteins. However, in strain Sterne, *BAS5207* is interrupted by two frameshift mutations (a single-base-pair insertion corresponding to nucleotide 1805 and a 14-bp insertion between nucleotides 5040 and 5041 in the *BAS5207* open reading frame [ORF]) and multiple deletions at the C terminus, leading us to conclude that *BAS5207* is likely a pseudogene in this strain. To construct a chromosomal insertion of *edsRS* into the pseudogene locus *BAS5207*, plasmid pLM4.*5207* was constructed as described above with the exception that the flanking region overlap site contained recognition sequences for the restriction nucleases NheI and KpnI. The *edsRS* genes were fused to the *eds* promoter by PCR-SOE, and the resulting product was inserted between the NheI and KpnI sites of pLM4.*5207* to generate a plasmid for chromosomal complementation of *edsRS*, pLM4.*edsRScomp*. Mutagenesis was performed using this vector as described previously (92) and confirmed by PCR and Sanger sequencing.

Expression studies. *B. anthracis* cultures were grown in LB at 37°C with shaking for 6 h (mid-log phase). Cultures were divided in half and then dosed with either DMSO control or 10 μg/ml targocil. Cultures were returned to 37°C for 10 min. Cultures were mixed at a 1:1 ratio with a 1:1 mixture of cold acetone and EtOH and stored at −80°C until RNA isolation. RNA was isolated using an RNeasy kit (Qiagen), and DNA was removed using a Turbo DNA-free kit (Invitrogen, Thermo Scientific). Quantification of RNA was performed using a Thermo Scientific NanoDrop spectrophotometer, and then cDNA was synthesized using an iScript cDNA synthesis kit (Bio-Rad). RNA sequencing was performed by Hudson-Alpha as described previously (93). qRT-PCR was performed as previously described using the threshold cycle ($\Delta\Delta^{-CT}$) method and iQ SYBR green Supermix (Bio-Rad) (94).

TABLE 2 Plasmids

Plasmid	Description	Reference or source
pLM4	Allelic exchange vector for *B. anthracis*	92
pLM4.*edsRS*	Vector to delete *edsRS*	This study
pLM4.*5207*	Vector to integrate genes within *BAS5207*	This study
pLM4.*edsRScomp*	Vector to integrate *edsRS* within *BAS5207*	This study
pLM4.*BAS1661-BAS1663clsT*	Vector to delete *BAS1661-BAS1663clsT*	This study
pOS1.P$_{lgt}$	Empty vector	92
pOS1.P$_{eds}$*xylE*	*xylE* reporter vector	This study
pOS1.P$_{lgt}$*edsRS*	*edsRS* complementation vector	This study
pOS1.P$_{lgt}$*clsT*	*clsT* complementation vector	This study

TABLE 3 Primers

Primer	Sequence	Use
edsRS KO XmaI fwd	GCATGACCCGGGATAGAAGTTTTACGTACATTTCG	Mutagenesis
edsRS KO SOE-L	CTTCCTTGGTACCTTATACCGCTTCCTGTCTTTTTC	Mutagenesis
edsRS KO SOE-R	CGGTATAAGGTACCAAGGAAGTTTACCTATGAATGG	Mutagenesis
edsRS KO SacI rev	GCATGAGAGCTCGTGCATACTTACTCACCATCC	Mutagenesis
5207 XmaI fwd	GCATGACCCGGGCTATGTAATTAGCTGGG	Chromosomal insertion
5207 SOE-L	GCTAGCGCATGCGGTACCGTTACTTTACCATCCGCACC	Chromosomal insertion
5207 SOE-R	GGTACCGCATGCGCTAGCGTTAAAGACTTGGAGCCTGG	Chromosomal insertion
5207 KO SacI rev	GCATGAGAGCTCCTTCATTCGTATCTCTATTAACG	Chromosomal insertion
edsRScomp KpnI fwd	GCATGAGGTACCTCGAATATATATCTTACCCG	Chromosomal complementation
edsRScomp SOE-L	CTTCTCTATCATCTCTCCACCCCCGCT	Chromosomal complementation
edsRScomp SOE-R	GGTGGAGAGATGATAGAGAAGAAGAGGATTG	Chromosomal complementation
edsRScomp NheI rev	GCATGAGAATTCGCTAGCGGACTATGTAACTAAGACGG	Chromosomal complementation
BAS1661-BAS1663clsT KO XmaI fwd	GCATGACCCGGGAAAGATATGCAGCGACTTACG	Mutagenesis
BAS1661-BAS1663clsT KO SOE-L	CAACCTTTATACCCCTATTTCGGTTTCTCTGC	Mutagenesis
BAS1661-BAS1663clsT KO SOE-R	CGAAATAGGGGTATAAAGGTTGATGGGAAAAGG	Mutagenesis
BAS1661-BAS1663clsT KO SacI rev	GCATGAGAGCTCGATGAGGCCATATAAACGTGTC	Mutagenesis
P*eds*xylE EcoRI fwd	GCATGAGAATTCTATCTTACCCGATTGTATCATG	Reporter
P*eds*xylE SOE-L	CTTTGTTCATCTCTCCACCCCCGCTG	Reporter
P*eds*xylE SOE-R	GGGTGGAGAGATGAACAAAGGTGTAATGCGAC	Reporter
P*eds*xylE BamHI rev	GCATGAGGATCCTCAGGTCAGCACGGTCATG	Reporter
P*lgt*edsRS fwd	CAATTGAGGTGAACATATGCTCGAGATGATAGAGAAGAAGAGGATTGAGATTTTTC	Complementation
P*lgt*edsRS rev	AAACACTACCCCCTTGTTTGGATCCTATCCATCCCTTTTCTTCC	Complementation
P*lgt*clsT fwd	CAATTGAGGTGAACATATGCTCGAGATGAACATGATTAAAAAAATATTGC	Complementation
P*lgt*clsT rev	AAACACTACCCCCTTGTTTGGATCCTTATAAATAAAAATCCACCATCC	Complementation
edsR fwd	TTTTGCTCCTGCCATAAGCC	qRT-PCR
edsR rev	CGCCCTGGATACTTTGAACG	qRT-PCR
edsS fwd	CCCTCACCCCATCTTTTCCT	qRT-PCR
edsS rev	ATGGAAATGGCATTCGTGGT	qRT-PCR
BAS1661 fwd	GCAAGAGTGGAGGAAGCACT	qRT-PCR
BAS1661 rev	CCAACTGTCGGCTCATCCAT	qRT-PCR
BAS1662 fwd	CAATGTAGCGGCCGAAGTTG	qRT-PCR
BAS1662 rev	TCGTCGTCATTACAACCGCA	qRT-PCR
BAS1663 fwd	GTAAAGTGGCAGGGACGGAT	qRT-PCR
BAS1663 rev	TCCTGATAAGTTCGCTGCTGA	qRT-PCR
clsT fwd	GAAGCGGCGTATCCATACAT	qRT-PCR
clsT rev	GCCCTACAATAGGACCACCA	qRT-PCR

Targocil toxicity growth curves. Strains of interest were streaked on LBA and grown at 30°C for 16 to 18 h. Single colonies were used to start cultures containing the same medium used for the assay as annotated and were grown for 16 h at 30°C with shaking. Cultures were diluted 1:100 into fresh media and grown with shaking for 6 h at 37°C. One microliter of each culture was added to 99 μl of LB or RPMI medium plus 1% Casamino Acids, as annotated, containing 0 to 100 μg/ml targocil in a 96-well flat-bottomed plate. Growth was monitored over time at 37°C by measuring the optical density at 600 nm in a BioTek Epoch2 spectrophotometer and analyzed in BioTek Gen5 software.

XylE assay. To monitor *eds* promoter activity, a XylE reporter plasmid was generated. In the pOS1 vector (95), the *eds* promoter (P*eds*) sequence was fused to *xylE* using PCR-SOE as described previously (96). This vector was carried through the cloning strains described above followed by electroporation into *B. anthracis*. Strains containing the P*eds*xylE reporter plasmid were grown at 37°C in LB containing chloramphenicol and 0 to 1 μg/ml targocil. After 6 h, the abundance of the XylE enzyme present in *B. anthracis* cellular lysates was assessed by measuring the rate at which catechol was converted to 2-hydroxymuconic acid using a spectrophotometer as described previously (58).

Spore preparation. Modified G medium (MGM) sporulation media were used for spore preparation (97). A single colony of *B. anthracis* was used to inoculate LB and grown for 4 h at 37°C with shaking. This culture was then back-diluted 1:20 into a flask containing MGM at a volume that provides maximum aeration. Cultures were then grown at 37°C for 72 h. The bacterial pellet was collected using centrifugation and washed repeatedly using sterile deionized water (diH$_2$O). After washing of the spores was performed a minimum of 4 times, the culture suspension was incubated at 65°C for 30 min. Samples were washed with sterile diH$_2$O again and then diluted and plated onto LB for quantification.

Spore outgrowth curves. Spores were prepared as described above. Enumerated spores were diluted to a concentration of 1×10^8 using diH$_2$O. One microliter of each spore preparation was added to 99 μl media containing 0 or 25 μg/ml targocil in a 96-well flat-bottomed plate. Growth was monitored over time at 37°C by measuring the optical density at 600 nm in a BioTek Epoch2 spectrophotometer and analyzed with BioTek Gen5 software.

Quantification of spore germination. Spores were prepared as described above. Enumerated spores were diluted to a concentration of 1×10^6 in LB broth containing a vehicle control or 100 μg/ml targocil. Cultures were incubated at 37°C for 5 min. Samples were dilution plated onto LB agar to

determine the total bacterial density. The same samples were then incubated at 65°C for 30 min to lyse vegetative cells. The boiled suspension was dilution plated to enumerate spore counts.

Disc diffusion assay. This assay was modified from studies previously described (98). Overnight cultures were grown at 30°C for 16 h. Following incubation, bacteria were mixed with top agar made from LB broth and poured onto LB agar plates. Sterile discs were placed onto the plates and loaded with one of each of the compounds included in our screening panel. The plates were incubated at 30°C for 18 h and then imaged. The diameter of the zone of inhibition was then measured. Experiments were performed twice.

Envelope permeability assay. Overnight cultures were grown at 30°C in RPMI medium plus 1% Casamino Acids with chloramphenicol. Cultures were normalized to an optical density at 600 nm (OD_{600}) of 0.3 in fresh media using a black-walled 96-well plate. The indicated treatments were added to the cultures and allowed to incubate at 37°C for 30 min. Ethidium bromide was added rapidly at 1 μg/ml, and the fluorescence (excitation [Ex], 530 nm; emission [Em], 600 nm) was immediately read kinetically using a BioTek Cytation 5 plate reader.

Cardiolipin relative quantification. Lipids were extracted from cell pellets (normalized by OD) using the Bligh-Dyer method (99). Extracts were dried under nitrogen and reconstituted in 100 μl of 65% acetonitrile–30% isopropyl alcohol–5% water. All samples contained 5 μg/ml of a cardiolipin standard [CL(16:0/18:1)] (Avanti Polar Lipids, Inc., Alabaster, AL, USA). A 15-μl volume of each sample was injected into an Acquity Arc ultra-high-performance liquid chromatography (UPLC) system (Waters Corporation, Milford, MA, USA). Lipids were separated using an Acquity UPLC HSS C_{18} column (Waters Corporation, Milford, MA, USA) with 1.8-μm particle size and dimensions of 2.1 mm by 150 mm. The aqueous solvent system (solvent A) consisted of 60% acetonitrile, 40% water, 0.1% formic acid, and 10 mM ammonium acetate. The organic solvent system (solvent B) consisted of 90% isopropyl alcohol, 10% acetonitrile, 10 mM ammonium acetate, and 0.1% formic acid (100). The following gradient was used: 0 min, 70% solvent A; 0 to 5 min, 70% to 57% solvent A; 5 to 5.1 min, 57% to 50% solvent A; 5.1 to 14 min, 50% to 30% solvent A; 14 to 21 min, 30% to 1% solvent A; 21 to 30 min, 1% solvent A; 30 to 30.1 min, 1% to 70% A. The column was allowed to equilibrate at 70% solvent A for 9.9 min prior to the next injection. The column heater was set at 40°C, and the flow rate was 0.22 ml/min. After separation, samples were introduced by electrospray ionization (2.5-kV capillary; 100°C source temperature; 40-V sampling cone) into a quadrupole-time of flight mass spectrometer (Waters Synapt G2-Si; Waters Corporation, Milford, MA, USA) for analysis in negative-ionization mode (trap and transfer collision energies, 15 V; resolution mode; ion mobility not enabled). Samples were analyzed in data-dependent mode with a survey window at mass-to-charge (*m/z*) ratios of 500 to 1,750 with a scan time of 0.2 s. Fragmentation data were acquired using a collision energy ramp of 6 to 147 eV (depending on the *m/z* value selected) with a 30-s exclusion window. The instrument was calibrated using sodium formate prior to analysis, and a lock spray containing a tuned mix of known *m/z* values (Agilent Technologies, Inc., Santa Clara, CA, USA) was infused (flow rate, 5 μl/min; scan time, 1 s; 10-s intervals; 3 scans averaged) during analysis for internal calibration of data postacquisition. Cardiolipin lipids eluted between 24 and 26 min. Data were analyzed by separately extracting ion chromatograms for all annotated cardiolipins within spectra obtained from parent strain samples. Peaks from extracted ion chromatograms were integrated manually and normalized to the area of the internal cardiolipin standard. Normalized areas were then summed for all annotated species. Data represent results from biological triplicates with two technical replicates each.

Data availability. RNA sequencing data were deposited in the Gene Expression Omnibus (GSE142363).

SUPPLEMENTAL MATERIAL

Supplemental material is available online only.

FIG S1, TIF file, 2.3 MB.
FIG S2, TIF file, 0.5 MB.
FIG S3, TIF file, 0.6 MB.
TABLE S1, DOCX file, 0.01 MB.
TABLE S2, DOCX file, 0.02 MB.
TABLE S3, DOCX file, 0.01 MB.
TABLE S4, DOCX file, 0.01 MB.

REFERENCES

1. Dixon TC, Meselson M, Guillemin J, Hanna PC. 1999. Anthrax. N Engl J Med 341:815–826. https://doi.org/10.1056/NEJM199909093411107.
2. Moran GJ. 1999. Bioterrorism alleging use of anthrax and interim guidelines for management--United States. Ann Emerg Med 34:229–232. https://doi.org/10.1016/S0196-0644(99)70237-4.
3. Mock M, Fouet A. 2001. Anthrax. Annu Rev Microbiol 55:647–671. https://doi.org/10.1146/annurev.micro.55.1.647.
4. Jernigan JA, Stephens DS, Ashford DA, Omenaca C, Topiel MS, Galbraith M, Tapper M, Fisk TL, Zaki S, Popovic T, Meyer RF, Quinn CP, Harper SA, Fridkin SK, Sejvar JJ, Shepard CW, McConnell M, Guarner J, Shieh WJ, Malecki JM, Gerberding JL, Hughes JM, Perkins BA, Anthrax Bioterrorism Investigation Team. 2001. Bioterrorism-related inhalational anthrax: the first 10 cases reported in the United States. Emerg Infect Dis 7:933–944. https://doi.org/10.3201/eid0706.010604.
5. Weir E. 2000. Anthrax: of bison and bioterrorism. CMAJ 163:608–608.
6. Mwakapeje ER, Hogset S, Fyumagwa R, Nonga HE, Mdegela RH, Skjerve E. 2018. Anthrax outbreaks in the humans - livestock and wildlife interface areas of Northern Tanzania: a retrospective record review 2006–2016. BMC Public Health 18:106. https://doi.org/10.1186/s12889-017-5007-z.
7. Hanczaruk M, Reischl U, Holzmann T, Frangoulidis D, Wagner DM, Keim PS, Antwerpen MH, Meyer H, Grass G. 2014. Injectional anthrax in heroin users, Europe, 2000-2012. Emerg Infect Dis 20:322–323. https://doi.org/10.3201/eid2002.120921.
8. Kamal SM, Rashid AK, Bakar MA, Ahad MA. 2011. Anthrax: an update. Asian Pac J Trop Biomed 1:496–501. https://doi.org/10.1016/S2221-1691(11)60109-3.
9. Alpuche Aranda CM, Swanson JA, Loomis WP, Miller SI. 1992. *Salmonella typhimurium* activates virulence gene transcription within acidified macrophage phagosomes. Proc Natl Acad Sci U S A 89:10079–10083. https://doi.org/10.1073/pnas.89.21.10079.
10. Fields PI, Groisman EA, Heffron F. 1989. A *Salmonella* locus that controls resistance to microbicidal proteins from phagocytic cells. Science 243:1059–1062. https://doi.org/10.1126/science.2646710.
11. Garcia Vescovi E, Soncini FC, Groisman EA. 1996. Mg2+ as an extracellular signal: environmental regulation of *Salmonella* virulence. Cell 84:165–174. https://doi.org/10.1016/s0092-8674(00)81003-x.
12. Wosten MM, Kox LF, Chamnongpol S, Soncini FC, Groisman EA. 2000. A signal transduction system that responds to extracellular iron. Cell 103:113–125. https://doi.org/10.1016/s0092-8674(00)00092-1.
13. Lina G, Jarraud S, Ji G, Greenland T, Pedraza A, Etienne J, Novick RP, Vandenesch F. 1998. Transmembrane topology and histidine protein kinase activity of AgrC, the agr signal receptor in *Staphylococcus aureus*. Mol Microbiol 28:655–662. https://doi.org/10.1046/j.1365-2958.1998.00830.x.
14. Aguilar PS, Hernandez-Arriaga AM, Cybulski LE, Erazo AC, de Mendoza D. 2001. Molecular basis of thermosensing: a two-component signal transduction thermometer in *Bacillus subtilis*. EMBO J 20:1681–1691. https://doi.org/10.1093/emboj/20.7.1681.
15. Mansilla MC, Aguilar PS, Albanesi D, Cybulski LE, Altabe S, de Mendoza D. 2003. Regulation of fatty acid desaturation in *Bacillus subtilis*. Prostaglandins Leukot Essent Fatty Acids 68:187–190. https://doi.org/10.1016/s0952-3278(02)00269-7.
16. Cybulski LE, del Solar G, Craig PO, Espinosa M, de Mendoza D. 2004. *Bacillus subtilis* DesR functions as a phosphorylation-activated switch to control membrane lipid fluidity. J Biol Chem 279:39340–39347. https://doi.org/10.1074/jbc.M405150200.
17. Albanesi D, Mansilla MC, de Mendoza D. 2004. The membrane fluidity sensor DesK of *Bacillus subtilis* controls the signal decay of its cognate response regulator. J Bacteriol 186:2655–2663. https://doi.org/10.1128/jb.186.9.2655-2663.2004.
18. Najle SR, Inda ME, de Mendoza D, Cybulski LE. 2009. Oligomerization of *Bacillus subtilis* DesR is required for fine tuning regulation of membrane fluidity. Biochim Biophys Acta 1790:1238–1243. https://doi.org/10.1016/j.bbagen.2009.07.002.
19. Bredeston LM, Marciano D, Albanesi D, De Mendoza D, Delfino JM. 2011. Thermal regulation of membrane lipid fluidity by a two-component system in *Bacillus subtilis*. Biochem Mol Biol Educ 39:362–366. https://doi.org/10.1002/bmb.20510.
20. Martin M, de Mendoza D. 2013. Regulation of *Bacillus subtilis* DesK

21. thermosensor by lipids. Biochem J 451:269–275. https://doi.org/10.1042/BJ20121825.
21. de Mendoza D. 2014. Temperature sensing by membranes. Annu Rev Microbiol 68:101–116. https://doi.org/10.1146/annurev-micro-091313-103612.
22. Inda ME, Vandenbranden M, Fernandez A, de Mendoza D, Ruysschaert JM, Cybulski LE. 2014. A lipid-mediated conformational switch modulates the thermosensing activity of DesK. Proc Natl Acad Sci U S A 111:3579–3584. https://doi.org/10.1073/pnas.1317147111.
23. Navarre WW, Schneewind O. 1999. Surface proteins of gram-positive bacteria and mechanisms of their targeting to the cell wall envelope. Microbiol Mol Biol Rev 63:174–229. https://doi.org/10.1128/MMBR.63.1.174-229.1999.
24. Giesbrecht P, Wecke J, Reinicke B. 1976. On the morphogenesis of the cell wall of staphylococci. Int Rev Cytol 44:225–318. https://doi.org/10.1016/s0074-7696(08)61651-4.
25. Beveridge TJ, Pouwels PH, Sara M, Kotiranta A, Lounatmaa K, Kari K, Kerosuo E, Haapasalo M, Egelseer EM, Schocher I, Sleytr UB, Morelli L, Callegari ML, Nomellini JF, Bingle WH, Smit J, Leibovitz E, Lemaire M, Miras I, Salamitou S, Beguin P, Ohayon H, Gounon P, Matuschek M, Koval SF. 1997. Functions of S-layers. FEMS Microbiol Rev 20:99–149. https://doi.org/10.1111/j.1574-6976.1997.tb00305.x.
26. Mesnage S, Tosi-Couture E, Gounon P, Mock M, Fouet A. 1998. The capsule and S-layer: two independent and yet compatible macromolecular structures in *Bacillus anthracis*. J Bacteriol 180:52–58. https://doi.org/10.1128/JB.180.1.52-58.1998.
27. Wessels MR, Rubens CE, Benedi VJ, Kasper DL. 1989. Definition of a bacterial virulence factor: sialylation of the group B *streptococcal* capsule. Proc Natl Acad Sci U S A 86:8983–8987. https://doi.org/10.1073/pnas.86.22.8983.
28. Lee K, Campbell J, Swoboda JG, Cuny GD, Walker S. 2010. Development of improved inhibitors of wall teichoic acid biosynthesis with potent activity against *Staphylococcus aureus*. Bioorg Med Chem Lett 20:1767–1770. https://doi.org/10.1016/j.bmcl.2010.01.036.
29. Molnar J, Pragai B. 1971. Attempts to detect the presence of teichoic acid in *Bacillus anthracis*. Acta Microbiol Acad Sci Hung 18:105–108.
30. Garufi G, Hendrickx AP, Beeri K, Kern JW, Sharma A, Richter SG, Schneewind O, Missiakas D. 2012. Synthesis of lipoteichoic acids in *Bacillus anthracis*. J Bacteriol 194:4312–4321. https://doi.org/10.1128/JB.00626-12.
31. Sterne M. 1946. Avirulent anthrax vaccine. Onderstepoort J Vet Sci Anim Ind 21:41–43.
32. Alex LA, Simon MI. 1994. Protein histidine kinases and signal transduction in prokaryotes and eukaryotes. Trends Genet 10:133–138. https://doi.org/10.1016/0168-9525(94)90215-1.
33. Swanson RV, Alex LA, Simon MI. 1994. Histidine and aspartate phosphorylation: two-component systems and the limits of homology. Trends Biochem Sci 19:485–490. https://doi.org/10.1016/0968-0004(94)90135-X.
34. Ducros VM, Lewis RJ, Verma CS, Dodson EJ, Leonard G, Turkenburg JP, Murshudov GN, Wilkinson AJ, Brannigan JA. 2001. Crystal structure of GerE, the ultimate transcriptional regulator of spore formation in *Bacillus subtilis*. J Mol Biol 306:759–771. https://doi.org/10.1006/jmbi.2001.4443.
35. Theodoulou FL, Kerr ID. 2015. ABC transporter research: going strong 40 years on. Biochem Soc Trans 43:1033–1040. https://doi.org/10.1042/BST20150139.
36. Campbell J, Singh AK, Swoboda JG, Gilmore MS, Wilkinson BJ, Walker S. 2012. An antibiotic that inhibits a late step in wall teichoic acid biosynthesis induces the cell wall stress stimulon in *Staphylococcus aureus*. Antimicrob Agents Chemother 56:1810–1820. https://doi.org/10.1128/AAC.05938-11.
37. Chien Y, Manna AC, Projan SJ, Cheung AL. 1999. SarA, a global regulator of virulence determinants in *Staphylococcus aureus*, binds to a conserved motif essential for sar-dependent gene regulation. J Biol Chem 274:37169–37176. https://doi.org/10.1074/jbc.274.52.37169.
38. Reizer J, Reizer A, Saier MH. Jr, 1992. A new subfamily of bacterial ABC-type transport systems catalyzing export of drugs and carbohydrates. Protein Sci 1:1326–1332. https://doi.org/10.1002/pro.5560011012.
39. Koonin EV. 1996. A duplicated catalytic motif in a new superfamily of phosphohydrolases and phospholipid synthases that includes poxvirus

envelope proteins. Trends Biochem Sci 21:242–243. https://doi.org/10.1016/S0968-0004(96)30024-8.

40. Tan BK, Bogdanov M, Zhao J, Dowhan W, Raetz CR, Guan Z. 2012. Discovery of a cardiolipin synthase utilizing phosphatidylethanolamine and phosphatidylglycerol as substrates. Proc Natl Acad Sci U S A 109:16504–16509. https://doi.org/10.1073/pnas.1212797109.

41. Terwilliger A, Swick MC, Pflughoeft KJ, Pomerantsev A, Lyons CR, Koehler TM, Maresso A. 2015. *Bacillus anthracis* overcomes an amino acid auxotrophy by cleaving host serum proteins. J Bacteriol 197:2400–2411. https://doi.org/10.1128/JB.00073-15.

42. Buyck JM, Plesiat P, Traore H, Vanderbist F, Tulkens PM, Van Bambeke F. 2012. Increased susceptibility of Pseudomonas aeruginosa to macrolides and ketolides in eukaryotic cell culture media and biological fluids due to decreased expression of oprM and increased outer-membrane permeability. Clin Infect Dis 55:534–542. https://doi.org/10.1093/cid/cis473.

43. Kumaraswamy M, Lin L, Olson J, Sun CF, Nonejuie P, Corriden R, Dohrmann S, Ali SR, Amaro D, Rohde M, Pogliano J, Sakoulas G, Nizet V. 2016. Standard susceptibility testing overlooks potent azithromycin activity and cationic peptide synergy against MDR *Stenotrophomonas maltophilia*. J Antimicrob Chemother 71:1264–1269. https://doi.org/10.1093/jac/dkv487.

44. Lin L, Nonejuie P, Munguia J, Hollands A, Olson J, Dam Q, Kumaraswamy M, Rivera H, Jr, Corriden R, Rohde M, Hensler ME, Burkart MD, Pogliano J, Sakoulas G, Nizet V. 2015. Azithromycin synergizes with cationic antimicrobial peptides to exert bactericidal and therapeutic activity against highly multidrug-resistant Gram-negative bacterial pathogens. EBioMedicine 2:690–698. https://doi.org/10.1016/j.ebiom.2015.05.021.

45. Moayeri M, Leppla SH, Vrentas C, Pomerantsev AP, Liu S. 2015. Anthrax pathogenesis. Annu Rev Microbiol 69:185–208. https://doi.org/10.1146/annurev-micro-091014-104523.

46. Drysdale M, Heninger S, Hutt J, Chen Y, Lyons CR, Koehler TM. 2005. Capsule synthesis by *Bacillus anthracis* is required for dissemination in murine inhalation anthrax. EMBO J 24:221–227. https://doi.org/10.1038/sj.emboj.7600495.

47. Brittingham KC, Ruthel G, Panchal RG, Fuller CL, Ribot WJ, Hoover TA, Young HA, Anderson AO, Bavari S. 2005. Dendritic cells endocytose *Bacillus anthracis* spores: implications for anthrax pathogenesis. J Immunol 174:5545–5552. https://doi.org/10.4049/jimmunol.174.9.5545.

48. Cleret A, Quesnel-Hellmann A, Vallon-Eberhard A, Verrier B, Jung S, Vidal D, Mathieu J, Tournier JN. 2007. Lung dendritic cells rapidly mediate anthrax spore entry through the pulmonary route. J Immunol 178:7994–8001. https://doi.org/10.4049/jimmunol.178.12.7994.

49. Haque MA, Russell NJ. 2004. Strains of *Bacillus cereus* vary in the phenotypic adaptation of their membrane lipid composition in response to low water activity, reduced temperature and growth in rice starch. Microbiology 150:1397–1404. https://doi.org/10.1099/mic.0.26767-0.

50. Epand RF, Savage PB, Epand RM. 2007. Bacterial lipid composition and the antimicrobial efficacy of cationic steroid compounds (Ceragenins). Biochim Biophys Acta 1768:2500–2509. https://doi.org/10.1016/j.bbamem.2007.05.023.

51. Dalebroux ZD, Edrozo MB, Pfuetzner RA, Ressl S, Kulasekara BR, Blanc MP, Miller SI. 2015. Delivery of cardiolipins to the *Salmonella* outer membrane is necessary for survival within host tissues and virulence. Cell Host Microbe 17:441–451. https://doi.org/10.1016/j.chom.2015.03.003.

52. Lonergan ZR, Nairn BL, Wang J, Hsu YP, Hesse LE, Beavers WN, Chazin WJ, Trinidad JC, VanNieuwenhze MS, Giedroc DP, Skaar EP. 2019. An *Acinetobacter baumannii*, zinc-regulated peptidase maintains cell wall integrity during immune-mediated nutrient sequestration. Cell Rep 26:2009–2018.e6. https://doi.org/10.1016/j.celrep.2019.01.089.

53. Kamischke C, Fan J, Bergeron J, Kulasekara HD, Dalebroux ZD, Burrell A, Kollman JM, Miller SI. 14 January 2019, posting date. The *Acinetobacter baumannii* Mla system and glycerophospholipid transport to the outer membrane. Elife https://doi.org/10.7554/eLife.40171.

54. Molohon KJ, Blair PM, Park S, Doroghazi JR, Maxson T, Hershfield JR, Flatt KM, Schroeder NE, Ha T, Mitchell DA. 2016. Plantazolicin is an ultra-narrow spectrum antibiotic that targets the *Bacillus anthracis* membrane. ACS Infect Dis 2:207–220. https://doi.org/10.1021/acsinfecdis.5b00115.

55. Zhang T, Muraih JK, Tishbi N, Herskowitz J, Victor RL, Silverman J, Uwumarenogie S, Taylor SD, Palmer M, Mintzer E. 2014. Cardiolipin prevents membrane translocation and permeabilization by daptomy-

cin. J Biol Chem 289:11584–11591. https://doi.org/10.1074/jbc.M114.554444.

56. El Khoury M, Swain J, Sautrey G, Zimmermann L, Van Der Smissen P, Décout J-L, Mingeot-Leclercq M-P. 2017. Targeting bacterial cardiolipin enriched microdomains: an antimicrobial strategy used by amphiphilic aminoglycoside antibiotics. Sci Rep 7:10697. https://doi.org/10.1038/s41598-017-10543-3.

57. de Been M, Francke C, Moezelaar R, Abee T, Siezen RJ. 2006. Comparative analysis of two-component signal transduction systems of *Bacillus cereus, Bacillus thuringiensis* and *Bacillus anthracis*. Microbiology 152:3035–3048. https://doi.org/10.1099/mic.0.29137-0.

58. Stauff DL, Skaar EP. 2009. *Bacillus anthracis* HssRS signalling to HrtAB regulates haem resistance during infection. Mol Microbiol 72:763–778. https://doi.org/10.1111/j.1365-2958.2009.06684.x.

59. Mike LA, Choby JE, Brinkman PR, Olive LQ, Dutter BF, Ivan SJ, Gibbs CM, Sulikowski GA, Stauff DL, Skaar EP. 2014. Two-component system cross-regulation integrates *Bacillus anthracis* response to heme and cell envelope stress. PLoS Pathog 10:e1004044. https://doi.org/10.1371/journal.ppat.1004044.

60. Gupta V, Chaudhary N, Aggarwal S, Adlakha N, Gulati P, Bhatnagar R. 2017. Functional analysis of BAS2108-2109 two component system: evidence for protease regulation in *Bacillus anthracis*. Int J Biochem Cell Biol 89:71–84. https://doi.org/10.1016/j.biocel.2017.06.004.

61. Dhiman A, Bhatnagar S, Kulshreshtha P, Bhatnagar R. 2014. Functional characterization of WalRK: a two-component signal transduction system from *Bacillus anthracis*. FEBS Open Bio 4:65–76. https://doi.org/10.1016/j.fob.2013.12.005.

62. Aggarwal S, Somani VK, Gupta V, Kaur J, Singh D, Grover A, Bhatnagar R. 2017. Functional characterization of PhoPR two component system and its implication in regulating phosphate homeostasis in *Bacillus anthracis*. Biochim Biophys Acta Gen Subj 1861:2956–2970. https://doi.org/10.1016/j.bbagen.2016.09.022.

63. Gupta V, Jain K, Garg R, Malik A, Gulati P, Bhatnagar R. 2018. Characterization of a two component system, Bas1213-1214, important for oxidative stress in *Bacillus anthracis*. J Cell Biochem 119:5761–5774. https://doi.org/10.1002/jcb.26751.

64. Chandramohan L, Ahn JS, Weaver KE, Bayles KW. 2009. An overlap between the control of programmed cell death in *Bacillus anthracis* and sporulation. J Bacteriol 191:4103–4110. https://doi.org/10.1128/JB.00314-09.

65. Tropp BE. 1997. Cardiolipin synthase from *Escherichia coli*. Biochim Biophys Acta 1348:192–200. https://doi.org/10.1016/s0005-2760(97)00100-8.

66. Ohta A, Obara T, Asami Y, Shibuya I. 1985. Molecular cloning of the cls gene responsible for cardiolipin synthesis in *Escherichia coli* and phenotypic consequences of its amplification. J Bacteriol 163:506–514. https://doi.org/10.1128/JB.163.2.506-514.1985.

67. Kawai F, Shoda M, Harashima R, Sadaie Y, Hara H, Matsumoto K. 2004. Cardiolipin domains in *Bacillus subtilis* Marburg membranes. J Bacteriol 186:1475–1483. https://doi.org/10.1128/jb.186.5.1475-1483.2004.

68. Eichenberger P, Jensen ST, Conlon EM, van Ooij C, Silvaggi J, Gonzalez-Pastor JE, Fujita M, Ben-Yehuda S, Stragier P, Liu JS, Losick R. 2003. The sigmaE regulon and the identification of additional sporulation genes in *Bacillus subtilis*. J Mol Biol 327:945–972. https://doi.org/10.1016/s0022-2836(03)00205-5.

69. Lopez CS, Alice AF, Heras H, Rivas EA, Sanchez-Rivas C. 2006. Role of anionic phospholipids in the adaptation of *Bacillus subtilis* to high salinity. Microbiology 152:605–616. https://doi.org/10.1099/mic.0.28345-0.

70. Helmann JD, Wu MF, Kobel PA, Gamo FJ, Wilson M, Morshedi MM, Navre M, Paddon C. 2001. Global transcriptional response of *Bacillus subtilis* to heat shock. J Bacteriol 183:7318–7328. https://doi.org/10.1128/JB.183.24.7318-7328.2001.

71. Tsai M, Ohniwa RL, Kato Y, Takeshita SL, Ohta T, Saito S, Hayashi H, Morikawa K. 2011. *Staphylococcus aureus* requires cardiolipin for survival under conditions of high salinity. BMC Microbiol 11:13. https://doi.org/10.1186/1471-2180-11-13.

72. Koprivnjak T, Zhang D, Ernst CM, Peschel A, Nauseef WM, Weiss JP. 2011. Characterization of *Staphylococcus aureus* cardiolipin synthases 1 and 2 and their contribution to accumulation of cardiolipin in stationary phase and within phagocytes. J Bacteriol 193:4134–4142. https://doi.org/10.1128/JB.00288-11.

73. Laganas V, Alder J, Silverman JA. 2003. In vitro bactericidal activities of daptomycin against *Staphylococcus aureus* and *Enterococcus faecalis* are not mediated by inhibition of lipoteichoic acid biosynthesis. Anti-

microb Agents Chemother 47:2682–2684. https://doi.org/10.1128/aac.47.8.2682-2684.2003.

74. Alborn WE, Jr, Allen NE, Preston DA. 1991. Daptomycin disrupts membrane potential in growing *Staphylococcus aureus*. Antimicrob Agents Chemother 35:2282–2287. https://doi.org/10.1128/aac.35.11.2282.

75. Silverman JA, Perlmutter NG, Shapiro HM. 2003. Correlation of daptomycin bactericidal activity and membrane depolarization in *Staphylococcus aureus*. Antimicrob Agents Chemother 47:2538–2544. https://doi.org/10.1128/aac.47.8.2538-2544.2003.

76. Kelesidis T, Humphries R, Uslan DZ, Pegues DA. 2011. Daptomycin nonsusceptible enterococci: an emerging challenge for clinicians. Clin Infect Dis 52:228–234. https://doi.org/10.1093/cid/ciq113.

77. Davlieva M, Zhang W, Arias CA, Shamoo Y. 2013. Biochemical characterization of cardiolipin synthase mutations associated with daptomycin resistance in enterococci. Antimicrob Agents Chemother 57:289–296. https://doi.org/10.1128/AAC.01743-12.

78. Palmer KL, Daniel A, Hardy C, Silverman J, Gilmore MS. 2011. Genetic basis for daptomycin resistance in enterococci. Antimicrob Agents Chemother 55:3345–3356. https://doi.org/10.1128/AAC.00207-11.

79. Coe KA, Lee W, Stone MC, Komazin-Meredith G, Meredith TC, Grad YH, Walker S. 2019. Multi-strain Tn-Seq reveals common daptomycin resistance determinants in *Staphylococcus aureus*. PLoS Pathog 15:e1007862. https://doi.org/10.1371/journal.ppat.1007862.

80. Swain J, El Khoury M, Kempf J, Briée F, Van Der Smissen P, Décout J-L, Mingeot-Leclercq M-P. 2018. Effect of cardiolipin on the antimicrobial activity of a new amphiphilic aminoglycoside derivative on *Pseudomonas aeruginosa*. PLoS One 13:e0201752. https://doi.org/10.1371/journal.pone.0201752.

81. Molohon KJ, Melby JO, Lee J, Evans BS, Dunbar KL, Bumpus SB, Kelleher NL, Mitchell DA. 2011. Structure determination and interception of biosynthetic intermediates for the plantazolicin class of highly discriminating antibiotics. ACS Chem Biol 6:1307–1313. https://doi.org/10.1021/cb200339d.

82. Cote CK, Van Rooijen N, Welkos SL. 2006. Roles of macrophages and neutrophils in the early host response to *Bacillus anthracis* spores in a mouse model of infection. Infect Immun 74:469–480. https://doi.org/10.1128/IAI.74.1.469-480.2006.

83. Hu H, Emerson J, Aronson AI. 2007. Factors involved in the germination and inactivation of *Bacillus anthracis* spores in murine primary macrophages. FEMS Microbiol Lett 272:245–250. https://doi.org/10.1111/j.1574-6968.2007.00766.x.

84. Russell BH, Vasan R, Keene DR, Xu Y. 2007. *Bacillus anthracis* internalization by human fibroblasts and epithelial cells. Cell Microbiol 9:1262–1274. https://doi.org/10.1111/j.1462-5822.2006.00869.x.

85. Sanz P, Teel LD, Alem F, Carvalho HM, Darnell SC, O'Brien AD. 2008. Detection of *Bacillus anthracis* spore germination in vivo by bioluminescence imaging. Infect Immun 76:1036–1047. https://doi.org/10.1128/IAI.00985-07.

86. Barua S, McKevitt M, DeGiusti K, Hamm EE, Larabee J, Shakir S, Bryant K, Koehler TM, Blanke SR, Dyer D, Gillaspy A, Ballard JD. 2009. The mechanism of *Bacillus anthracis* intracellular germination requires multiple and highly diverse genetic loci. Infect Immun 77:23–31. https://doi.org/10.1128/IAI.00801-08.

87. Guidi-Rontani C, Levy M, Ohayon H, Mock M. 2002. Fate of germinated *Bacillus anthracis* spores in primary murine macrophages. Mol Microbiol 42:931–938. https://doi.org/10.1046/j.1365-2958.2002.02874.x.

88. Hood MI, Skaar EP. 2012. Nutritional immunity: transition metals at the pathogen-host interface. Nat Rev Microbiol 10:525–537. https://doi.org/10.1038/nrmicro2836.

89. Mellman I, Fuchs R, Helenius A. 1986. Acidification of the endocytic and exocytic pathways. Annu Rev Biochem 55:663–700. https://doi.org/10.1146/annurev.bi.55.070186.003311.

90. Kim HS, Sherman D, Johnson F, Aronson AI. 2004. Characterization of a major *Bacillus anthracis* spore coat protein and its role in spore inactivation. J Bacteriol 186:2413–2417. https://doi.org/10.1128/jb.186.8.2413-2417.2004.

91. Horton RM, Cai ZL, Ho SN, Pease LR. 1990. Gene splicing by overlap extension: tailor-made genes using the polymerase chain reaction. Biotechniques 8:528–535.

92. Kern JW, Schneewind O. 2008. BslA, a pXO1-encoded adhesin of *Bacillus anthracis*. Mol Microbiol 68:504–515. https://doi.org/10.1111/j.1365-2958.2008.06169.x.

93. Juttukonda LJ, Green ER, Lonergan ZR, Heffern MC, Chang CJ, Skaar EP. 19 December 2019, posting date. *Acinetobacter baumannii* OxyR regulates the transcriptional response to hydrogen peroxide. Infect Immun https://doi.org/10.1128/IAI.00413-18.

94. Choby JE, Grunenwald CM, Celis AI, Gerdes SY, DuBois JL, Skaar EP. 2018. *Staphylococcus aureus* HemX modulates glutamyl-tRNA reductase abundance to regulate heme biosynthesis. mBio 9:e02287-17. https://doi.org/10.1128/mBio.02287-17.

95. Schneewind O, Model P, Fischetti VA. 1992. Sorting of protein A to the staphylococcal cell wall. Cell 70:267–281. https://doi.org/10.1016/0092-8674(92)90101-h.

96. Torres VJ, Stauff DL, Pishchany G, Bezbradica JS, Gordy LE, Iturregui J, Anderson KL, Dunman PM, Joyce S, Skaar EP. 2007. A *Staphylococcus aureus* regulatory system that responds to host heme and modulates virulence. Cell Host Microbe 1:109–119. https://doi.org/10.1016/j.chom.2007.03.001.

97. Bergman NH, Anderson EC, Swenson EE, Janes BK, Fisher N, Niemeyer MM, Miyoshi AD, Hanna PC. 2007. Transcriptional profiling of *Bacillus anthracis* during infection of host macrophages. Infect Immun 75:3434–3444. https://doi.org/10.1128/IAI.01345-06.

98. Juttukonda LJ, Berends ETM, Zackular JP, Moore JL, Stier MT, Zhang Y, Schmitz JE, Beavers WN, Wijers CD, Gilston BA, Kehl-Fie TE, Atkinson J, Washington MK, Peebles RS, Chazin WJ, Torres VJ, Caprioli RM, Skaar EP. 2017. Dietary manganese promotes staphylococcal infection of the heart. Cell Host Microbe 22:531–542.e8. https://doi.org/10.1016/j.chom.2017.08.009.

99. Bligh EG, Dyer WJ. 1959. A rapid method of total lipid extraction and purification. Can J Biochem Physiol 37:911–917. https://doi.org/10.1139/o59-099.

100. Narváez-Rivas M, Zhang Q. 2016. Comprehensive untargeted lipidomic analysis using core–shell C30 particle column and high field orbitrap mass spectrometer. J Chromatogr A 1440:123–134. https://doi.org/10.1016/j.chroma.2016.02.054.

101. Kreiswirth BN, Löfdahl S, Betley MJ, O'Reilly M, Schlievert PM, Bergdoll MS, Novick RP. 1983. The toxic shock syndrome exotoxin structural gene is not detectably transmitted by a prophage. Nature 305:709–712. https://doi.org/10.1038/305709a0.

102. Novick RP. 1991. Genetic systems in staphylococci. Methods Enzymol 204:587–636. https://doi.org/10.1016/0076-6879(91)04029-n.